

Image Processing Methods for the Automated Assessment of Neuronal Outgrowth

Nicolas Gaborel¹, Jonathan Le Gall¹, Marwa El Bouz¹, Virginie Buhé¹, Ayman Alfalou¹, Laurent Misery², Anthony Courtois³, Bertrand Thollas³,
Dominique Paul¹

¹L@bISEN, Yncrea Ouest, 20 Rue Cuirassé Bretagne, 29200 Brest, France

²LNB (Laboratoire de Neurosciences de Brest), Université Bretagne Occidentale, 22, rue Camille Desmoulins, 29238 Brest, France

³Polymaris, 29200 Brest, France

Corresponding Author: Marwa El Bouz

Abstract: Neuronal outgrowth assessment is useful to understand the development of peripheral or central neurons and their regeneration after wounding. It consists in the determination of the length of the cell extensions (neurite length) using photos of neuron cultures. As the manual determination of neurite length is time-consuming and operator-dependent, many semi- or fully-automated methods have been developed. Most of them have been designed to analyze fluorescence microscopy images which allow clear delineation of cell bodies and neurites from the background. In this paper, we propose a new easy-to-use fully automated computer vision method based on denoising, background subtraction, edge and envelope detection, and designed to analyze compressed images (JPEG format) of non-fluorescent living neurons. A statistical tool was also integrated in the program to provide turnkey data to biologists. The reliability of our program was tested using images of differentiated PC-12 cell culture. Statistical analysis showed non-significant difference between the manual determination and our automated method.

Keywords: Light microscopy, image processing, living sensory neurons, neurite length, automatic processing, statistical analysis tool.

Date of Submission: 15-04-2019

Date of acceptance: 30-04-2019

I. Introduction

Neuronal growth assessment may be helpful in all neurobiology fields, such as the central nervous system development and the connectome understanding, or for the study of the sensory neuron development and regeneration after wounding. In the skin nerve endings permit the perception of temperature, pain, pruritus and touch and take part in skin homeostasis [1]. They may be responsible for abnormal sensations (paresthesia) occurring in various conditions when they are altered (sensitive skin, wound healing, etc.) [2, 3]. Therefore, there is a growing interest in the protection of these sensory neurons and in the development of products to alleviate the symptoms of paresthesia. In that context, neuriteogenesis assays have been developed to assess the neuronal outgrowth in the absence or in the presence of cosmetic and pharmaceutical ingredients, growth factors, and neurotoxic agents.

Differentiated PC-12 cells and primary neurons are frequently used as neuron models of neuriteogenesis [4, 5]. At the end of the *in vitro* culture of those cells, photos are usually taken to determine the neurite length using software such as ImageJ [6-9]. The major difficulty of this manual image analysis method lies in the laborious neurite detection and tracing within the whole neuron network visible on each picture. Furthermore, neurites are often ramified and the total length is much harder to assess. As a consequence, the manual determination of neurite length is very time-consuming and operator-dependent while an automated method quickly produces reproducible results.

A number of approaches to measuring neurite outgrowth have been designed [10-14], most of them work with fluorescence microscopy images: a previous fluorescent DNA labelling by DAPI or Hoechst associated with a specific cytoskeleton immunolabeling helps to respectively delineate the nucleus and the cytoplasm from the background [9, 13-18]. Other methods also use images acquired through phase-contrast microscopes [19-21]. All of these methods yield reliable results and overall, were designed with friendly and easy-to-use graphical user interfaces (GUI) for biologists. Nevertheless, these methods have the disadvantage of using fixed (killed) neurons to allow fluorescent detection, inducing additional costs, especially in the case of kinetic assays. To overcome these constraints, we developed a new program designed to work with images

acquired using light microscopy and JPEG lossy image format, still frequently used in biology. Our program is centered around an interface geared towards batch processing, outputting measurements in comma-separated values (csv) files to maximize automatization. It also includes a statistical analysis tool that ensures the data follows a normal distribution before making comparisons.

To validate our fully-automated method for the assessment of neurite length, we worked with differentiated PC-12 cells previously cultured with and without sulfated exopolysaccharides. The algorithmic results were compared to those obtained using the manual measuring method. This article is organized as follows: first we present the experimental conditions and the manual measure technique, we then delve into the steps that form the computer vision based method for measuring neurites. We conclude with statistical analysis of the two methods and discuss the results.

II. Image Acquisition & Manual Determination

2.1 PC-12 cell culture

Proliferating PC-12 cells (ATCC, Teddington, United Kingdom) were seeded at $7.9 \cdot 10^3$ cells per cm^2 in 12-well microplates and maintained at 37°C in a humidified atmosphere containing 5% CO_2 . They were cultured for the first day in Dulbecco's Minimum Essential Medium F-12 (DMEM-F12, LONZA, Basel, Switzerland). Then, the medium was removed and replaced by DMEM-F12 supplemented with HC, NGF to induce the neuronal differentiation of the PC-12 cells. Two days later, this medium was renewed and an EPS dilution or an equal volume of phosphate-buffered saline (PBS) was added to each well. Each culture condition was performed in duplicate.

2.2 Exopolysaccharides

Two lyophilized exopolysaccharides (EPS) provided by Polymaris Biotechnology (Brest, France) were tested: EPS 15 and EPS 268. They were dissolved at 1% w/v in sterile water to perform stock solutions. Each EPS was added to differentiated PC-12 cells at a final concentration of 100 $\mu\text{g}/\text{mL}$ or 10 $\mu\text{g}/\text{mL}$. The effect of EPS on the neurite outgrowth was evaluated after a 2-day incubation.

2.3 Neurite outgrowth assessment and acquisition

Differentiated living PC-12 cells were observed and photographed using a DLSR camera fitted on an inverted optical microscope (respectively E-510 and CKX41, Olympus, Tokyo, Japan). About eight to eleven photos were randomly taken per well, depending on the PC-12 cells distribution and the proportion of isolated neurites. Photos were 1600x1200 pixels JPEG images with an RGB color profile. They were analyzed with the ImageJ image processing program (NIH, Bethesda, MD, USA): segmented lines were traced following up the path of isolated neurites and their lengths were measured in pixel count to assess the neurite lengths. If applicable, the total length of ramifications was added to that of the corresponding neurites. Results were exported to a csv file for data analysis.

2.4 Automated method for neurite outgrowth assessment

The PC-12 cell culture images used to develop this method were those taken to carry out the previous manual determination. Each color channel, separately or combined, does not provide more information than the black and white conversion of the image; this is why all the treatment in the algorithm is done to the black and white version of the images. The successive steps of the method are described in the following section.

III. Computer Vision Based Method

3.1 Image preprocessing

Given the variability in image quality and background content (noise and defects, **figure 1.a**), the first treatment step consists of optimizing the photograph's contrast and filtering part of the noise. This is done for two reasons: to allow for better edge detection and to have accurate thresholds for binarizing the images.

First, a local contrast adjustment is performed, followed by local Gaussian filtering (local Laplacian filter [22]) to increase contrast and smooth the background (effectively removing most of the defects) while keeping the edges intact (**figure 1.b**). This step is necessary to increase the number of detections in the edge processing part of the algorithm, additionally, if the defects (parasite streaks and grooves in the background) are not removed, they are detected as neurites.

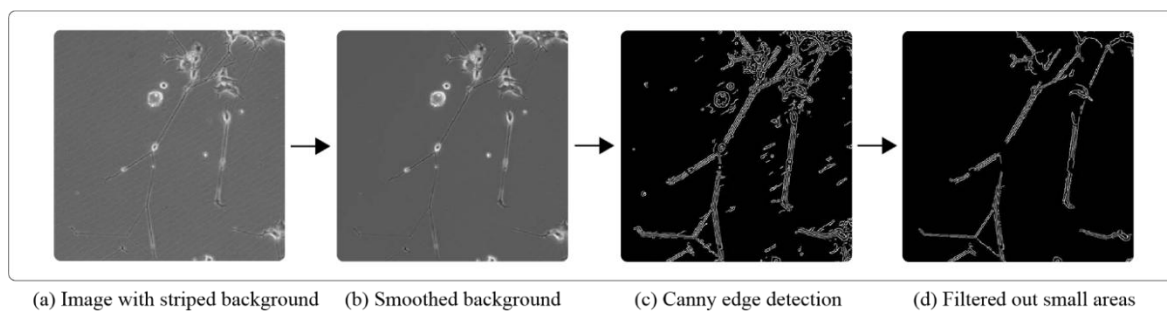


Figure 1 -Denoising and edge detection

To find an appropriate threshold for each image (an intensity value with which to binarize the image), images need to have a consistent intensity throughout. This problem becomes apparent with images showing the edges of the culture wells: dark circular areas form and throw off the mean intensity values (**figure 2.a**), meaning a part of the image would be ignored if simple thresholding was applied. In addition, either the image has what we consider a normal aspect, or it is too bright, with neurites and cell bodies showing opposite color intensities and contrasts. To palliate both problems, we extract the picture's background through approximation and Gaussian smoothing (**figure 2.b**) and we balance the original image with the result. For bright images, the background is completely subtracted, for "normal" images, 25% of the background is subtracted (**figure 2.c**).

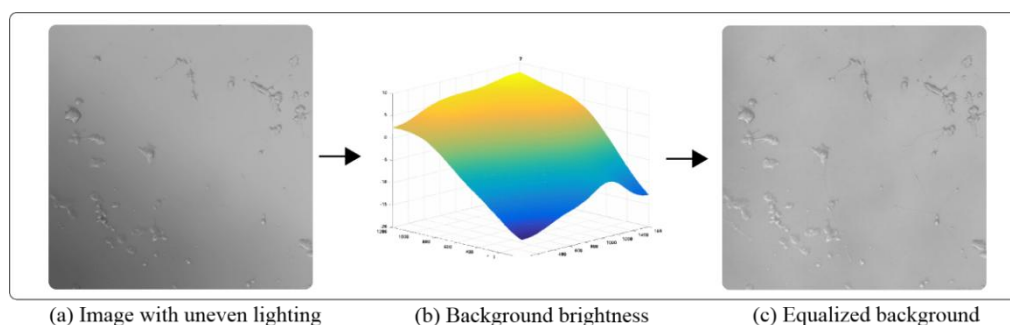


Figure 2 - Background estimation and subtraction

3.2 Edge detection

Once the images are enhanced and present less noise, the different items of interest may be isolated. To detect the neurites and the cell bodies, Canny's edge detection method is used [23, 24] because it outputs continuous lines and, in our case, provides better detection results than Sobel or Prewitt methods. This produces lines describing most of the shapes in the image: the neurites, cell bodies and some background noise (**figure 1.c**). With this technique, several lines are generated for a single edge and additional lines wrap and overlap in the cell bodies. To eliminate the noise detected after the Canny process, pixel clusters with a small (empirical) number of elements are removed. Results are filtered once more to discard the lines presenting a high eccentricity factor (curvature), thus removing only cell bodies (**figure 1.d**).

3.3 Envelope detection

To isolate and completely erase the cell bodies from the image, leaving only the neurites (**figure 4.a**), the binarized version of the photograph is used (**figure 3.a**). A threshold is computed from mean intensities so as to keep only the cell bodies (in the images used, neurites are dark and cell bodies have a white "glow" around them). To smooth and close the gaps in the shapes, the convex hull of each cell body is calculated [25], providing an envelope around the detected areas; the resulting shape is then dilated to ensure that the whole region is appropriately covered (**figure 3.b**). If the whole cell body region is not removed from the edge-detected image, lines that do not represent neurites will be processed and will inadequately contribute to the length measurements.

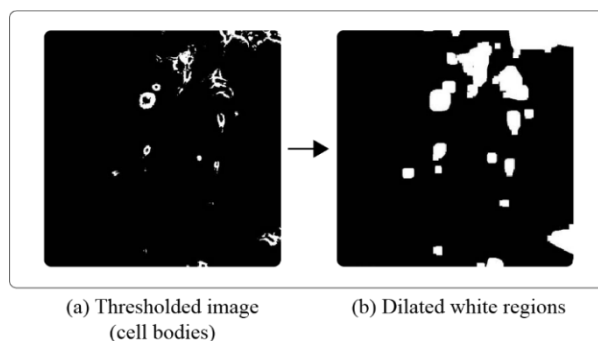


Figure 3 - Thresholding and dilation to isolate cell bodies

3.4 Edge Processing

Once edge detection has been applied and cell bodies have been removed from the image, the remaining lines can be processed (**figure 4.a**). To identify individual neurites, neighboring lines are grouped with an 8-pixel range (an empirical range suited to the image definition and neuron density of the culture wells). Connected and adjoining lines are given a label (a number from 0 to the maximum number of grouped shapes), these can then be displayed with a color gradient for debug and development purposes. Removing the cell bodies from the edge-detected image cuts part of the lines, producing small bundles of parasite pixels. These are filtered out by removing labels containing a small number of elements.

Afterwards, labeled lines are thickened to form continuous blobs, tripled or quadrupled contiguous lines become one. These expanded shapes are skeletonized [26] with the aim of reducing them to single lines describing the neurites. The presence of multiple sets of labeled lines offsets the skeletonization process and produces up to two roughly parallel lines. Another operation of dilation and skeletonization yields the expected results. Effectively, two iterations of the dilation and skeletonization process are applied to reach the final result (**figure 4.b**). Each detected neurite, with its ramifications, is measured by summing the white pixels contained in the associated label. These results are tallied in a matrix and exported in a csv (comma-separated values) file compatible with software like Microsoft Excel or MATLAB. In addition, the calculated lines are superimposed on the original photograph and shown next to the program interface; photos in a batch treatment stack up, allowing the operator to check the results once the process is completed (**figure 4.c**).

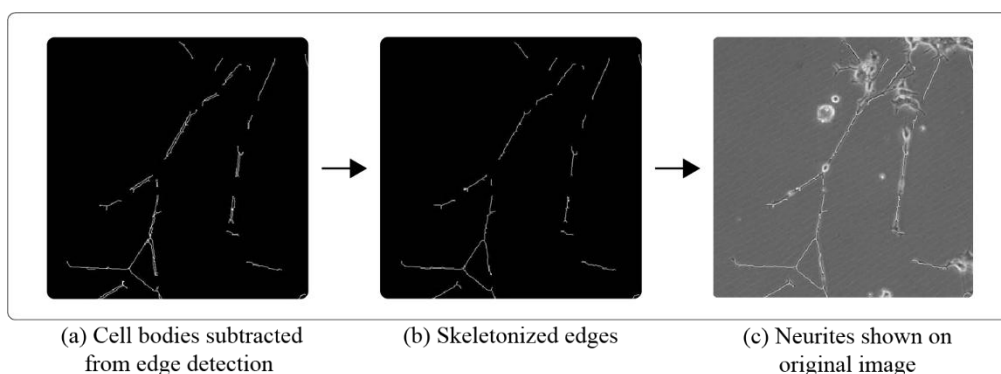


Figure 4 - Neurite skeletonization process

IV. Theory

To allow the program to make meaningful comparisons between samples and to produce accurate statistical results, the sets of measures from the csv files (with populations well over 100 elements) should approximately follow a normal distribution. To find out if our samples follow such a distribution, a chi-square test with 5% risk [27] is used. Manual counts as well as automated counts for our culture well images all failed the tests (**figure 5.a**), meaning the null hypothesis that the datasets follow a normal distribution was rejected with 5% risk. To use relevant tests such as Student/Welch tests, it is therefore necessary to classify (segment) the data in every set (**figure 5.b**). Segmentation is automatically performed if the program concludes that the datasets do not follow a normal distribution. Segmented sets all pass the chi-square test with 5% risk.

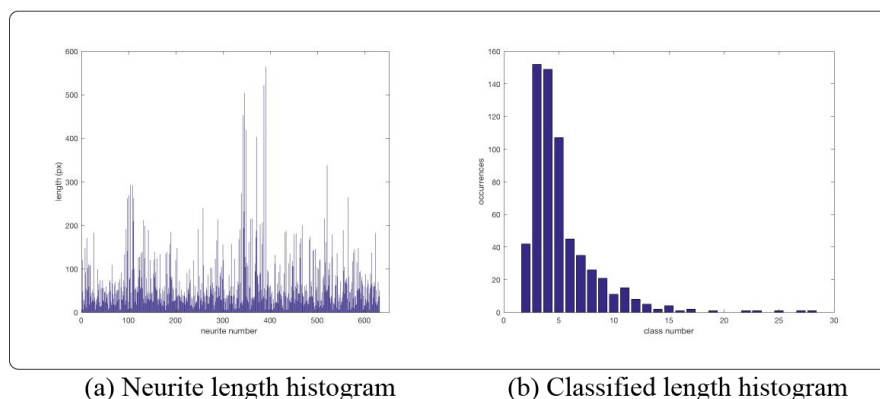


Figure 5 - Data normalization

On the newly-obtained datasets (which follow a distribution that can be approximated to a normal distribution thanks to the high sample population), length means need to be compared to assess the substances' impact on neuron development. To compare sample means, Student tests are usually conducted; however, such a test requires sample sizes and variances to be equal, which is not the case for our datasets. This is why Welch's t-tests (with 5% risk) are used to judge of mean equality. Mean neurite length differences may tell us whether the global growth was affected or not.

V. Results

5.1 Experimental results

This sub-section reports the results that allow us to conclude vis-à-vis the efficiency of our automated method. Firstly, the potential discrepancies between duplicate culture wells need to be assessed for each chemical. A significant difference between duplicates suggests an experimental error. Once the duplicate compliances are validated, their measurements can be pooled together to form denser datasets for statistical analysis.

The average neurite length and the statistical analysis results for the manual method and for the computer vision method of assessment are summarized in **table 1** (a and b). Culture well 1 is tested against well 2 with Welch t-tests. The resulting p-value may be used to draw a conclusion concerning mean equality. For our purposes, with a 5% risk, we conclude that all means are equal throughout the tests. The computer vision based results allow us to reach the same conclusions as the manual method when comparing mean length for the control PBS and the EPS. The mean length measures from the operator stand around 80 pixels while the means from the algorithm are in the vicinity of 50 pixels, consistently lower throughout the tests. This can be due to the fact that neurite bases are cropped when the algorithm discards cell bodies from the image.

5.2 Discussion

The assessment of neuronal outgrowth is essential in *in vitro* experiments using peripheral or central neuron cultures. In the skin, the development of sensory neurons is necessary to achieve proper development of the whole organ, and a loss in epidermal nerve fibers decreases the epidermal thickness [1]. Thus, the cosmetic and pharmaceutical industries show a growing interest for the protection and the regeneration of the epidermal nerve endings. The determination of the protective or the soothing effects of ingredients is assessed by culturing neurons with the molecules of interest and determining the neurite lengths, which reflects neuronal health.

The manual determination of the neurite lengths is quite robust but highly time-consuming. Given the significant number of candidate molecules and the multiple dose-response assays required for each one, the development of automated determination methods is needed. Although many methods have been developed, we propose a new one based on the automatic recognition and measurement of neurites from neuron culture JPEG photos without prior fluorescent staining to delineate the cell bodies and the nerve fibers from the background. One of its advantages is that it requires no user setup prior to use, there are no extra skills that the operator needs to acquire in order to properly use the software. In addition, manual neurite counts are extremely operator-dependent, the strength of the algorithm lies in the reproducibility of the results it gives and the speed at which it gives them. The program we developed takes about 30 seconds per image depending on neurite density. Thus, the operator can now simply check the resulting images once the process is over. The recorded measurements are then ready to be imported in software such as Microsoft Excel for further analysis. Alternatively, a statistical analysis feature is available on the graphical user interface (GUI), allowing on one hand to pool together duplicate culture wells if necessary and on the other hand, to automatically classify (normalize) and test datasets for mean and variance differences, offering a complete set of tools for assessing neuronal development.

The program developed here is aimed at processing compressed and noisy (background defects) images taken without expensive equipment. Software such as HCA-Vision [17], FluoroSNNAP [28], and NeuriteTracer [13] for ImageJ offer automated solutions for measuring neurites. The results they give are usually very accurate but their detection methods are based on fluorescent photography. Complete packages can be found in products like BioTek's Lionheart FX, proposing fluorescent microscopy coupled with image analysis. Fluorescent images are ideal for image processing, allowing to clearly distinguish areas of interest, but it is an expensive technique that requires fixing (therefore killing) the cells. Software using phase contrast microscope images [19-21] for automated neurite counts exist but require equipment that labs may not have. One very versatile program allows its users to treat light microscopy images: CellProfiler [29], but it appears that it was not designed to measure neurites.

Because of the JPEG compression, background noise and the geometry of the culture wells (giving rise to edge effects darkening the photos), image optimization (preprocessing) is an unavoidable step and adds to the total runtime of the program. Neurite shape is quite inconsistent, rendering line detection techniques like Hough's [30] ineffective; the tests we conducted with this method yielded unreliable and impractical results. Frequency analysis of the images such as edge detection through high frequencies was equally inconclusive because of the JPEG compression and noise. Edge detection with Canny algorithms (providing edges with continuous lines) is still the most appropriate for our problem [23, 24] and gave more accurate results compared to Sobel or Prewitt methods. Neurites are detected in a satisfying way in the first phase of the program, but in the cell body detection phase, part of the growth cones are cropped out to suppress surrounding noise. Since this is done throughout all the images, length proportion remains similar. It is also worth noting that our algorithm was tailored to detect neurites for PC12-cell cultures seeded at a $7.9 \cdot 10^3$ cells per cm^2 density.

VI. Conclusion

We have taken advantage of MATLAB's computing power to obtain an adaptable code able to deal with images presenting background noise and inhomogeneous light exposure as well as a variety of neurite and cell body shapes. This algorithm should reduce the time biologists spend measuring neurites in culture wells. With a 2012 2.3 GHz Intel i7 processor, the total treatment of a 5-photo batch takes around 140 seconds (an implementation with libraries such as OpenCV would significantly reduce the processing time). Photos may come from experiments with non-fluorescent living neurons and standard visible-light cameras; no additional investment is required from the lab.

Reference

- [1]. S.-T. Hsieh, W.-M. Lin, Modulation of Keratinocyte Proliferation by Skin Innervation, *Journal of Investigative Dermatology*. 113 (1999) 579–586. doi:10.1046/j.1523-1747.1999.00737.x.
- [2]. V. Buhé, Pathophysiological study of sensitive skin, *Acta Dermato Venereologica*. 96 (2016) 314–318.
- [3]. Laverdet B, Danigo A, Girard D, Magy L, Demiot C, Desmoulière A, Skin innervation: important roles during normal and pathological cutaneous repair, *Histology and Histopathology*. (2015) 875–892. doi:10.14670/HH-11-610.
- [4]. N.M. Radio, W.R. Mundy, Developmental neurotoxicity testing in vitro: Models for assessing chemical effects on neurite outgrowth, *NeuroToxicology*. 29 (2008) 361–376. doi:10.1016/j.neuro.2008.02.011.
- [5]. E.J. Calabrese, Enhancing and Regulating Neurite Outgrowth, *Critical Reviews in Toxicology*. 38 (2008) 391–418. doi:10.1080/10408440801981981.
- [6]. L. Ulmann, J.-L. Rodeau, L. Danoux, J.-L. Contet-Audonneau, G. Pauly, R. Schlichter, Trophic effects of keratinocytes on the axonal development of sensory neurons in a coculture model: Effect of keratinocytes on sensory neuron growth, *European Journal of Neuroscience*. 26 (2007) 113–125. doi:10.1111/j.1460-9568.2007.05649.x.
- [7]. N. Lebonvallet, J.-P. Pennec, C. Le Gall, U. Pereira, N. Boulais, J. Cheret, C. Jeanmaire, L. Danoux, G. Pauly, L. Misery, Effect of human skin explants on the neurite growth of the PC12 cell line, *Experimental Dermatology*. 22 (2013) 224–225. doi:10.1111/exd.12095.
- [8]. M.-J. Ahn, G.-W. Cho, Metformin promotes neuronal differentiation and neurite outgrowth through AMPK activation in human bone marrow-mesenchymal stem cells: Metformin Promotes Neurite Outgrowth through AMPK, *Biotechnology and Applied Biochemistry*. 64 (2017) 836–842. doi:10.1002/bab.1584.
- [9]. E. Meijering, M. Jacob, J.-C.F. Sarria, P. Steiner, H. Hirling, M. Unser, Design and validation of a tool for neurite tracing and analysis in fluorescence microscopy images, *Cytometry*. 58A (2004) 167–176. doi:10.1002/cyto.a.20022.
- [10]. Siriphorn, A, Chompoopong, S, & Tilokskulchai, K, The neurite outgrowth measurement of dorsal root ganglia explants cultured on estrogen and schwann cell-conditioned medium by using image analysis, *Siriraj Medical Journal*. 61 (2009).
- [11]. N.M. Radio, J.M. Breier, T.J. Shafer, W.R. Mundy, Assessment of Chemical Effects on Neurite Outgrowth in PC12 cells Using High Content Screening, *Toxicological Sciences*. 105 (2008) 106–118. doi:10.1093/toxsci/kfn114.
- [12]. P. Ramm, Y. Alexandrov, A. Cholewinski, Y. Cybuch, R. Nadon, B.J. Soltys, Automated Screening of Neurite Outgrowth, *Journal of Biomolecular Screening*. 8 (2003) 7–18. doi:10.1177/1087057102239779.
- [13]. M. Pool, J. Thiemann, A. Bar-Or, A.E. Fournier, NeuriteTracer: A novel ImageJ plugin for automated quantification of neurite outgrowth, *Journal of Neuroscience Methods*. 168 (2008) 134–139. doi:10.1016/j.jneumeth.2007.08.029.
- [14]. S.-Y. Ho, C.-Y. Chao, H.-L. Huang, T.-W. Chiu, P. Charoenkwan, E. Hwang, NeurphologyJ: An automatic neuronal morphology quantification method and its application in pharmacological discovery, *BMC Bioinformatics*. 12 (2011) 230. doi:10.1186/1471-2105-12-230.
- [15]. G. Pani, W.H. De Vos, N. Samari, L. de Saint-Georges, S. Baatout, P. Van Oostveldt, M.A. Benotmane, MorphoNeuroNet: An automated method for dense neurite network analysis: MorphoNeuroNet, *Cytometry Part A*. 85 (2014) 188–199. doi:10.1002/cyto.a.22408.

[16]. A.J. Haas, S. Prigent, S. Dutertre, Y. Le Dréan, Y. Le Page, Neurite analyzer: An original Fiji plugin for quantification of neuritogenesis in two-dimensional images, *Journal of Neuroscience Methods*. 271 (2016) 86–91. doi:10.1016/j.jneumeth.2016.07.011.

[17]. P. Vallotton, R. Lagerstrom, C. Sun, M. Buckley, D. Wang, M. De Silva, S.-S. Tan, J.M. Gunnensen, Automated analysis of neurite branching in cultured cortical neurons using HCA-Vision, *Cytometry Part A*. 71A (2007) 889–895. doi:10.1002/cyto.a.20462.

[18]. K.H. Ong, J. De, L. Cheng, S. Ahmed, W. Yu, NeuronCyto II: An automatic and quantitative solution for crossover neural cells in high throughput screening: Automatic Quantification of Crossed Neurites, *Cytometry Part A*. 89 (2016) 747–754. doi:10.1002/cyto.a.22872.

[19]. D. Gaublumme, T. Buyens, L. Moons, Automated Analysis of Neurite Outgrowth in Mouse Retinal Explants, *Journal of Biomolecular Screening*. 18 (2013) 534–543. doi:10.1177/1087057112471989.

[20]. O. Al-Kofahi, R.J. Radke, B. Roysam, G. Banker, Automated Semantic Analysis of Changes in Image Sequences of Neurons in Culture, *IEEE Transactions on Biomedical Engineering*. 53 (2006) 1109–1123. doi:10.1109/TBME.2006.873565.

[21]. H. Hartmann, K. Hoehne, E. Rist, A.M. Louw, B. Schlosshauer, miR-124 disinhibits neurite outgrowth in an inflammatory environment, *Cell and Tissue Research*. 362 (2015) 9–20. doi:10.1007/s00441-015-2183-y.

[22]. S. Paris, S.W. Hasinoff, J. Kautz, Local Laplacian filters: edge-aware image processing with a Laplacian pyramid, *Communications of the ACM*. 58 (2015) 81–91. doi:10.1145/2723694.

[23]. Raman Maini, Himanshu Aggarwal, Study and Comparison of Various Image Edge Detection Techniques, *International Journal of Image Processing (IJIP)*. 3 (2009).

[24]. Nadernejad, E, Sharifzadeh, S, & Hassanpour, H, Edge detection techniques: Evaluations and comparison, *Applied Mathematical Sciences*. 2 (2008) 1507–1520.

[25]. Govan, A, Introduction to optimization, North Carolina State University, SAMSI NDHS. (2006).

[26]. D. Attali, Squelettes et graphes de Voronoï 2D et 3D, phdthesis, Université Joseph-Fourier - Grenoble I, 1995. <https://tel.archives-ouvertes.fr/tel-00346066/document> (accessed July 3, 2018).

[27]. Saporta, G, Probabilités, analyse des données et statistique, Editions Technip, 2006.

[28]. T. Patel, FLUOROSNNAP, (2015).

[29]. Carpenter, A, CellProfiler: image analysis software for identifying and quantifying cell phenotypes, *Genome Biology*. (2006).

[30]. Milgram, M, Reconnaissance des formes: méthodes numériques et connexionnistes, A. Colin, 1993.

Table 1 a & b

Table 1 a

Well 1	Well 2	Mean neurite length [well 1] (px)	Mean neurite length [well 2] (px)	Welch t-test p-value
Duplicate wells comparison				
PBS	PBS	51.91	47.94	0.6743
EPS150.1%	EPS150.1%	52.86	47.72	0.2637
EPS15 1%	EPS15 1%	58.29	37.01	0.4515
EPS268 0.1%	EPS268 0.1%	52.96	51.79	0.0941
EPS268 1%	EPS268 1%	43.59	50.02	0.8049
Reference (PBS) vs. test chemical				
PBS [pooled]	EPS15 0.1% [pooled]	49.69	49.04	0.7845
PBS [pooled]	EPS15 1% [pooled]	49.69	49.59	0.9654
PBS [pooled]	EPS268 0.1% [pooled]	49.69	52.30	0.2918
PBS [pooled]	EPS268 1% [pooled]	49.69	47.17	0.2464

Table 1 b

Well 1	Well 2	Mean neurite length [well 1] (px)	Mean neurite length [well 2] (px)	Welch t-test p-value
Duplicate wells comparison				
PBS	PBS	77.02	86.65	0.9888
EPS150.1%	EPS150.1%	65.57	70.21	0.8417
EPS15 1%	EPS15 1%	78.89	67.04	0.1676
EPS268 0.1%	EPS268 0.1%	72.19	85.64	0.5811
EPS268 1%	EPS268 1%	69.50	69.07	0.9950
Reference (PBS) vs. test chemical				
PBS [pooled]	EPS15 0.1% [pooled]	82.07	68.10	0.5487
PBS [pooled]	EPS15 1% [pooled]	82.07	73.78	0.9683
PBS [pooled]	EPS268 0.1% [pooled]	82.07	77.53	0.7856
PBS [pooled]	EPS268 1% [pooled]	82.07	69.28	0.6718

Nicolas Gaborel. "Image Processing Methods for the Automated Assessment of Neuronal Outgrowth" *IOSR Journal of Computer Engineering (IOSR-JCE)* 21.2 (2019): 49-55.